Geological Magazine

www.cambridge.org/geo

Rapid Communication

Cite this article: Barrenechea JF, Borruel-Abadía V, Galán-Abellán AB, López-Gómez J, Esterle J, McCann T, de la Horra R, Ronchi A, Gianolla P, Luque FJ, Rossi VM, Paterson N, Smith RMH, Wolvaardt D, Brookfield ME, Bourquin S, and Ubide T. Latitude affects continental acidity in the Smithian–Spathian boundary biotic crisis. *Geological Magazine* **163**(e2): 1–8. https://doi.org/10.1017/S0016756825100472

Received: 24 July 2025
Revised: 4 December 2025
Accepted: 8 December 2025

Keywords:
Acidity; Smithian–Spathian; APS minerals; latitude; continental

Corresponding author:
Jose F. Barrenechea; Email: barrene@ucm.es

Latitude affects continental acidity in the Smithian–Spathian boundary biotic crisis

José F. Barrenechea[1,2], Violeta Borruel-Abadía[3], Ana Belén Galán-Abellán[4], José López-Gómez[2], Joan Esterle[5], Tom McCann[6], Raúl de la Horra[3], Ausonio Ronchi[7], Piero Gianolla[8], Francisco Javier Luque[1,2], Valentina M. Rossi[9], Niall Paterson[10], R.M.H. Smith[11,12], Derick Wolvaardt[11], Michael E. Brookfield[13], Sylvie Bourquin[14] and Teresa Ubide[5]

[1]Depto. Mineralogía y Petrología, Fac. Geología, Universidad Complutense de Madrid, Madrid, Spain; [2]Instituto de Geociencias (UCM, CSIC), Madrid, Spain; [3]Depto. Geodinámica, Estratigrafía y, Paleontología, Fac. Geología, Universidad Complutense de Madrid, Madrid, Spain; [4]Depto. Geología y Geoquímica, Fac. de Ciencias, Universidad Autónoma de Madrid, Madrid, Spain; [5]School of the Environment, The University of Queensland, Brisbane, QLD, Australia; [6]Institut für Geowissenschaften - Geologie/Sedimentologie, Universität Bonn, Bonn, Germany; [7]Dipto. di Scienze della Terra e dell'Ambiente, Università degli studi di Pavia, Pavia, Italy; [8]Dipto. di Fisica e Scienze della Terra, Ferrara, Italy; [9]Institute of Geosciences and Georesources, Pavia, Italy; [10]CASP, Cambridge, UK; [11]Evolutionary Studies Institute, University of the Witwatersrand, Johannesburg, South Africa; [12]Karoo Palaeontology, Iziko South African Museum, Cape Town, South Africa; [13]Jackson School of Geosciences, University of Texas at Austin, Austin, TX, USA and [14]Université de Rennes, CNRS, Géosciences Rennes, Rennes, France

Abstract

The extent to which continental acidity during the Early Triassic varied with latitude remains insufficiently constrained, despite its relevance for understanding environmental stress and biotic recovery patterns across the Smithian–Spathian boundary (SSB). We examined the abundance, textures and compositions of strontium-rich hydrated aluminium phosphate–sulphate (APS) minerals in 179 continental samples spanning tropical to high paleolatitudes in both hemispheres. APS minerals display broadly comparable early-diagenetic features across sections, indicating formation shortly after deposition under acidic meteoric conditions. Their distribution suggests a latitudinal trend: APS contents commonly exceed 0.1 vol.% in equatorial western peri-Tethyan basins, where faunal and floral records are sparse during the SSB, whereas concentrations decrease towards higher latitudes and are rare beyond ~40° in both hemispheres. This pattern does not appear to correlate with lithological or textural variability and may reflect spatial differences in the intensity or duration of acidification linked to Siberian Traps volcanism. Equatorial basins thus likely experienced more prolonged or recurrent acidic episodes, whereas higher-latitude areas may have been subject to comparatively attenuated effects, potentially contributing to earlier ecological recovery. These results provide a useful framework for evaluating continental acidification and its environmental implications during the interval following the end-Permian mass extinction (EPME).

1. Introduction

The end-Permian mass extinction (EPME) and the subsequent prolonged recovery were primarily triggered by the massive volcanic activity of the Siberian Traps magmatism (STM) (Svensen *et al.* 2009). This volcanism released immense quantities of greenhouse gases, sulphur compounds and halogens in rapid, repeated pulses that destabilized global environments. On land, the principal kill mechanisms included intense acid rain, ozone layer destruction leading to elevated UV-B radiation, mercury poisoning and abrupt global warming (Black *et al.* 2014; Li *et al.* 2022; Liu *et al.* 2023; Dal Corso *et al.* 2024). These stresses caused the widespread collapse of terrestrial ecosystems and a prolonged delay in ecological recovery (Galfetti *et al.* 2007; Stanley, 2009). Direct evidence for acidification and its latitudinal control on land during the EPME is, however, very scarce (Wu *et al.* 2024). The effects of the STM that triggered the EPME (Payne *et al.* 2004; Wignall, 2011) lasted until the end of the Early Triassic due to different intense pulses in activity (Svensen *et al.* 2009). The biotic crisis of the Smithian–Spathian boundary (SSB) was the result of one of these volcanic pulses and one of the last barriers to the onset of biotic recovery after the EPME (Galfetti *et al.* 2007; Payne *et al.* 2004; Posenato, 2019; Sahney and Benton, 2008).

During the last decade, SSB research constrained the effects of acidity on continental basins near the equator and the possible relationship between acidity and the circulation of volcanic aerosols due to global wind circulation (Galán-Abellán et al. 2013*a*; Borruel-Abadía *et al.* 2016, 2019; Barrenechea *et al.* 2025). In this study, we present new data from a global latitudinal

reconstruction of the acidity conditions in continental environments for the SSB, based on the quantification of strontium-rich hydrated aluminium phosphate–sulphate (APS) minerals that typically precipitate at low pH conditions (Dill, 2001; Stofreggen and Alpers, 1987). The results reveal a global pattern of environmental stress that could have emanated latitudinal from the uneven distribution of aerosols derived from STM.

1.a. Geological context

The Early Triassic (~251.9 to ~247.2 Ma) was characterized by three large-scale negative shifts in $\delta^{13}C$ ratios in marine carbonates (Payne *et al.* 2004). These excursions have been linked to episodes of massive CO_2 outgassing from the STM that likely produced ocean acidification, global warming and widespread anoxia/euxinia, with the largest occurring near the SSB. This latter episode also coincided with the extinction of ammonites and conodonts (Orchard, 2007) and impeded complete biotic recovery during the Early Triassic (Sahney and Benton, 2008).

On land, these pulses correlate with similar excursions reported from paleosol data (Retallack, 2021), with a drastic modification in the spore-pollen assemblages (Galfetti *et al.* 2007). In the continental realm, the massive release of CO_2 and other volcanic greenhouse gases from the STM generated sustained global warming and acid rain. In addition, episodic pyroclastic eruptions caused further sulphuric acid rain and ozone depletion, which in turn may have severely damaged the global environment, leading to the terrestrial biotic crisis (Black *et al.* 2014; Li *et al.* 2022; Dal Corso *et al.* 2024). Furthermore, Paterson *et al.* (2024) report increased concentrations of As, Co, Hg and Ni, which is interpreted as compelling evidence for heavy metal-induced stress and genetic disturbance in plant communities during the EPME. The SSB activity of the STM is widely considered to have the most severe paleoenvironmental effects in the Early Triassic (Retallack *et al.* 2011). In this context, the presence of APS minerals in continental rocks can provide insight into the environmental conditions that prevailed during the SSB crisis and the biotic recovery that followed. These minerals belong to the alunite supergroup and are stable under conditions of high $(PO_4)^{3-}$ activity, high oxygen potential and relatively low pH values (Dill, 2001; Vieillard *et al.* 1979; Stoffregen and Alpers, 1987). As recently shown in the SSB continental rocks of the W peri-Tethys, where APS formation is texturally constrained to follow the sedimentation process, relative proportions of APS minerals could reflect the duration and intensity of the acidification process (Barrenechea *et al.* 2025; Borruel-Abadía *et al.* 2016, 2019). Here, we address the acidity peaks that occurred on land during the SSB globally, encompassing several new locations at different latitudes.

2. Methods

We selected Smithian–Spathian sequences across a wide paleolatitude range, including nine outcrop sections and three drill cores (Figure 1). This selection completes previous detailed studies on a much larger number of sections in the Iberian Basin, the Catalan Basin – Minorca (Spain), the Nurra Basin (Sardinia, Italy) and the Western Dolomites (Vicentinian Prealps, Italy) (Barrenechea *et al.* 2025; Borruel Abadía *et al.* 2016, 2019; Galán-Abellán *et al.* 2013a). A total of 179 fine-grained sandstone samples were analysed, mostly of continental origin, but also from transitional to shallow marine environment in one drill core (Figure 2 and Supplementary material). All our sections are temporally and spatially constrained

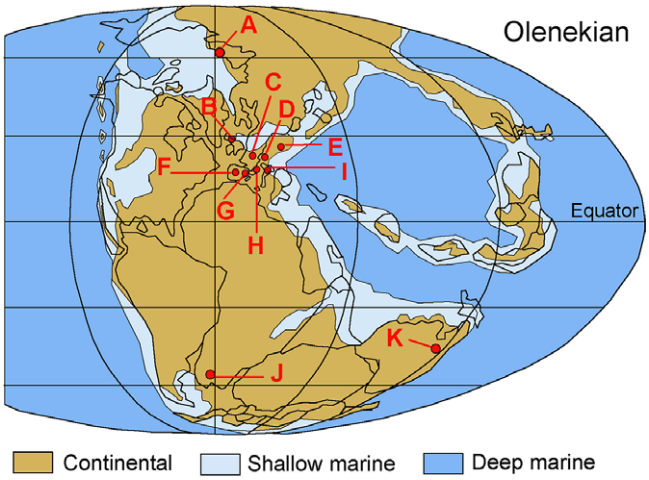

Figure 1. Pangea during the Olenekian, which includes the Smithian and the Spathian. A to K: location of the outcrop sections and drill cores of Figure 2.

based on terrestrial palynomorph and tetrapod assemblages or magnetostratigraphy. The sedimentary facies for the studied subunits are similar across all stratigraphic sections (Table S1, Supplementary material), indicating the distribution of APS and organic preservation are not facies-dependent. Most of the studied successions correspond to siliciclastic rocks, and only the section of the Western Dolomites (Italy) shows layers of carbonate rocks towards the top of the section.

The chemical composition of APS minerals was analysed with an electron microprobe analyser (EMPA) JEOL JXA-8900 M WDS. We quantified APS minerals based on EMPA elemental maps following the methodology of Borruel-Abadía *et al.* (2016). Textural relationships were described using a JEOL 6400 scanning electron microscope (SEM), equipped with an energy-dispersive spectrometer (EDS). Additional data on texture and composition of the samples were obtained in a TESCAN Vega 4 SEM (high/low vacuum) operating at 20 kV with colour cathodoluminescence and two EDX Bruker detectors (30 and 60 mm^2).

3. Results and discussion

When present, APS minerals show very similar textural and compositional characteristics in the different sections studied (Figure 3). They occur as small (0.2–5 μm), disseminated, euhedral, pseudocubic crystals or as polycrystalline aggregates (up to 200 μm). Their idiomorphic nature and delicate stepped faces rule out a detrital origin. Textural relationships indicate that the precipitation of diagenetic quartz and illite cement postdates the formation of APS minerals and suggests the replacement of metamorphic rock fragments and detrital micas occurred before the main stage of compaction of the sedimentary pile. All these features were first described in detail in many sections in the Iberian Ranges (Spain) by Galán-Abellán *et al.* (2013*a*) and were later reported in the Catalan Coastal Range, Minorca (Spain), Sardinia (Italy) (Borruel-Abadía *et al.* 2016) and the Western Dolomites (Italy) (Barrenechea *et al.* 2025). They concluded that APS minerals formed during early-diagenetic stages, shortly after sedimentation and most likely under the influence of acidic meteoric waters.

Our results show a clear latitudinal control on the concentration of APS minerals (Figure 4 and Supplementary Table S2). This cannot be ascribed to variations in grain size since all studied

https://doi.org/10.1017/S0016756825100472 Published online by Cambridge University Press

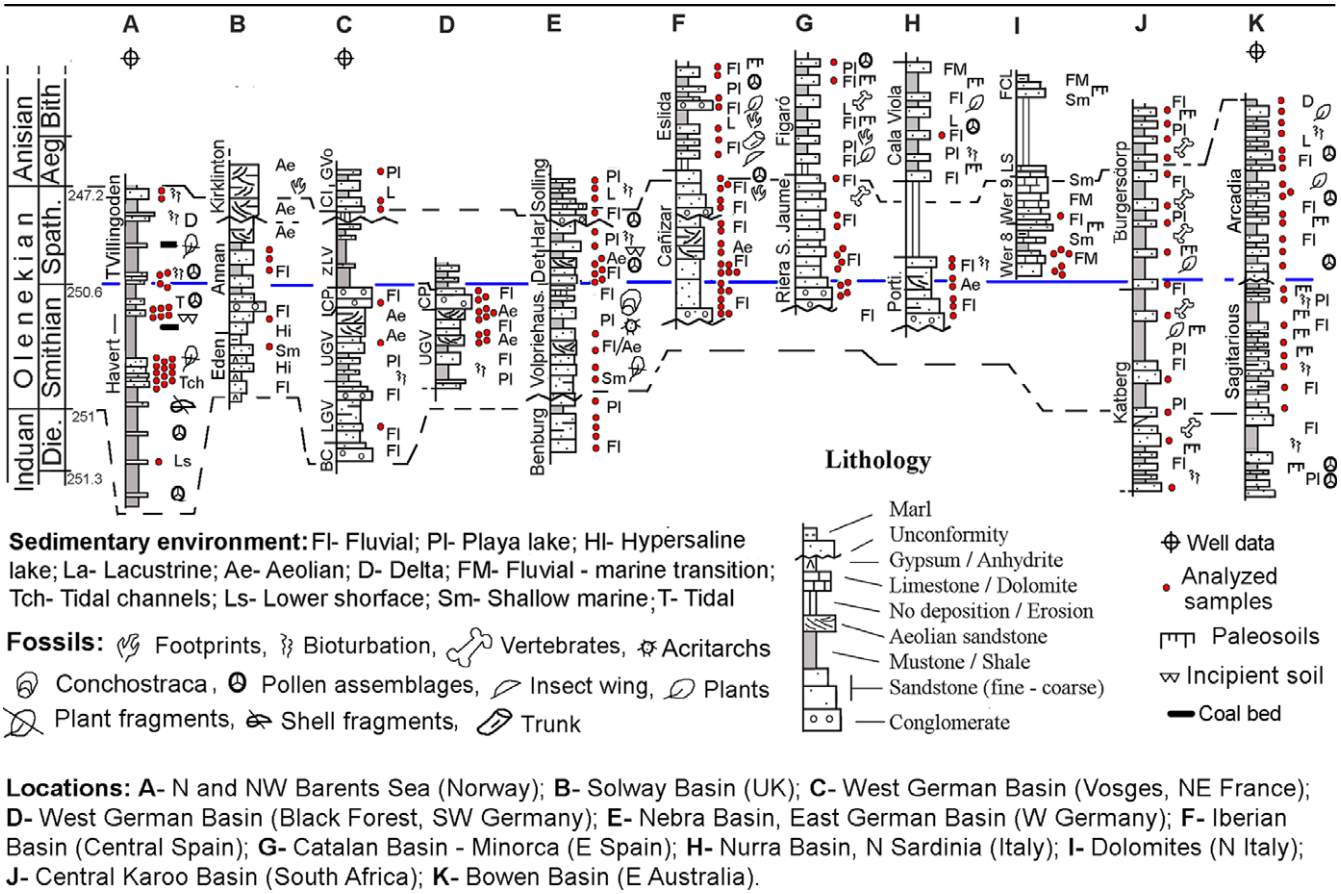

Figure 2. Studied logs and drill cores (A to K). See locations in Figure 1. There is no vertical scale. (See data on the location of the samples and authors of the studied sections in the Complementary Information to Figure 2, Supplementary Material).

sequences are lithologically and texturally similar. The formation of APS minerals primarily depends on acidic conditions, which in turn may have been favoured by a warm, seasonal climate. Although Galán-Abellán *et al.* (2013*b*) suggested that pyrite oxidation could enhance acidity, they also considered a potential contribution from volcanic aerosols. While isotopic data confirming a volcanic origin for these aerosols are lacking, the remarkable textural and compositional uniformity of APS across sections separated by thousands of kilometres indicates a common formation mechanism operating at a scale broader than strictly local. Furthermore, the absence of carbonate layers in most of the studied sites suggests a limited influence of their potential buffering capacity against the low pH induced by volcanic inputs of acidic gases. In fact, this influence should only be considered in the Western Dolomites section, which contains carbonate layers, but the APS minerals are found only in the siliciclastic strata of fluvial origin (Supplementary Table S1). On the other hand, sections with sporadic marine influence may have been affected by the buffering effect of seawater, which could bias the interpretation of the presence of APS minerals as indicators of increased acidity. We consider it unlikely that this buffering effect influences the decreasing trend in APS mineral contents towards higher latitudes, given the overall predominance of continental facies in these sections. However, it cannot be ruled out that it may have some impact on the successions with greater marine influence.

Across the SSB, contents greater than 0.1 vol.% are detected around the equatorial zones, in the W peri-Tethys basins, while the concentration of these minerals decreases drastically towards higher latitudes, being practically non-existent from 40º N and 40º S onwards. In the W peri-Tethys, trends in the APS minerals are consistent in all outcrop sections and drill cores (Figure 4). APS variations through time are also clear. The oldest studied samples have low concentrations in APS minerals but increase substantially across the SSB in all studied basins (from 0.09 to 1.07 vol.%) (Figure 4 and Supplementary Table S2). The highest APS mineral contents are observed in the Iberian Basin, central Spain, located near the equator, about 10º N–14º N (Borruel-Abadía *et al.* 2016), where no remains of fauna or flora have been found so far in the Smithian–Spathian sedimentary record (Borruel-Abadía *et al.* 2019). Such high APS mineral levels persist until the late Spathian, where bioturbation processes appear as first signs of life recovery. In the lower-middle Anisian successions, APS mineral percentages are low in this basin (between 0.006 and 0.09 vol.%), and this decrease coincides with the first occurrence of paleosols, bioturbations, plant remains, tetrapod footprints and insects (Borruel-Abadía *et al.* 2015) (Figure 4). A similar trend occurs in Sardinia (Italy), in latitudes similar to Iberia, where high APS mineral content (0.04–0.18 vol.%) also coincides with the absence of flora and fauna during the SSB, and the first signs of life appear only in the late Spathian (Baucon *et al.* 2014). In a recent work, Barrenechea *et al.* (2025) report the same pattern of APS mineral distribution with respect to the lack of indicators of organic activity in the Western Dolomites, also in sub-equatorial latitudes. The absence of fossils in these continental W peri-Tethys areas also coincides with extreme temperatures and hyperarid environmental conditions (Bourquin *et al.* 2011).

https://doi.org/10.1017/S0016756825100472 Published online by Cambridge University Press

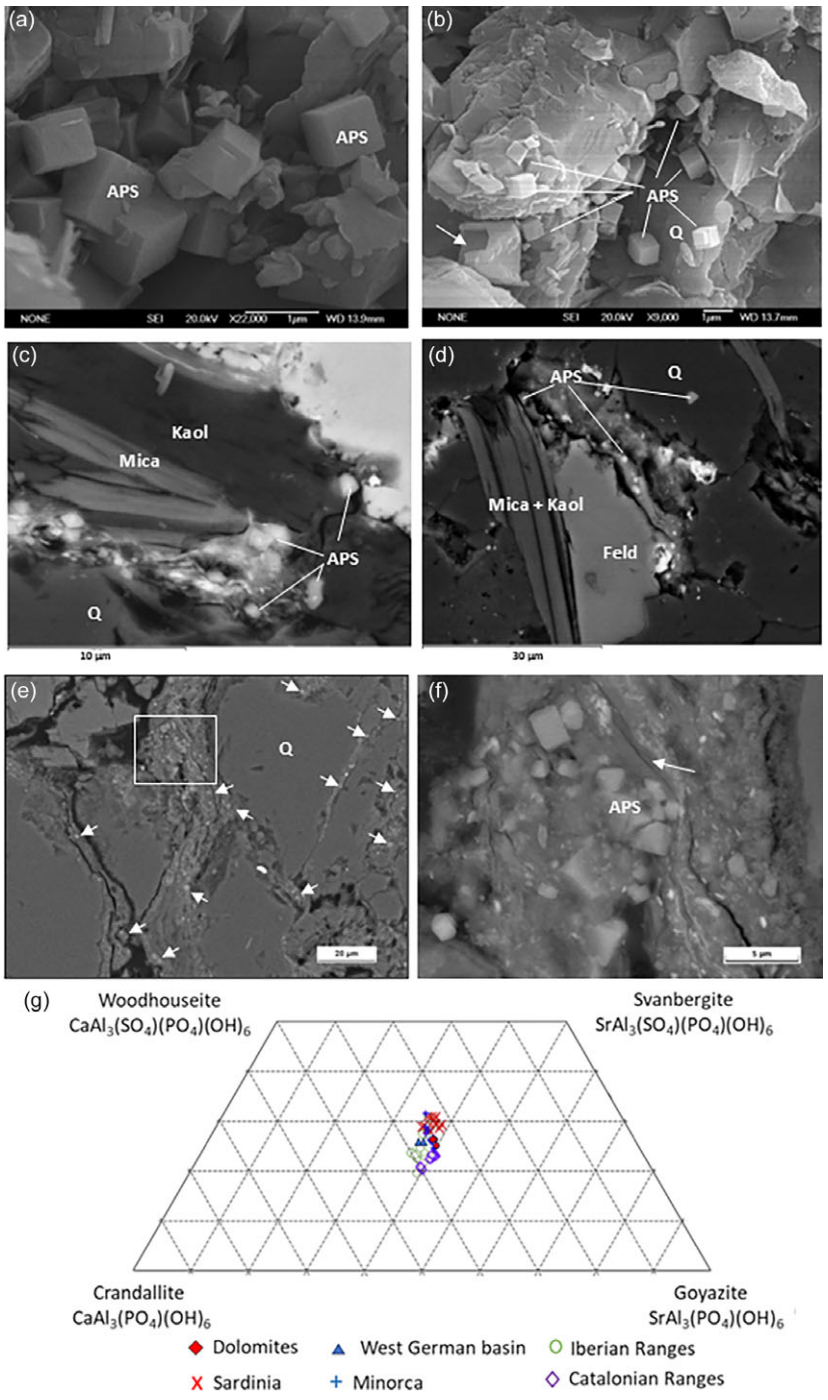

Figure 3. Scanning electron microscopy (SEM) images from sample MG7 (Dolomites, Italy): (a) euhedral crystals of APS minerals surrounded by quartz and illite. (b) APS crystals and moulds within the quartz cement (white arrow). (c) Backscattered electron (BSE) image in a thin section of sample MG1, with small APS minerals and detrital mica plates replaced by kaolinite. (d) Kaolinized mica with disseminated APS minerals. (e) BSE image of a thin section of sample V48 (W German basin). The white arrows point to APS mineral crystals in the clay matrix. (f) Enlarged view of crystals of APS minerals, closely related to the kaolinized detrital mica (white arrow). (g) Plot of APS mineral compositions from Dolomites and from the W German basin compared to previously published data from other peri-Tethyan basins. Q: quartz; Feld: feldspar; Kaol: kaolinite; APS: APS mineral.

Towards higher latitudes, the APS mineral content drops rapidly (Figure 4). Rare disseminated crystals occur in samples near the SSB in NE France and central Germany, with a maximum APS mineral concentration of 0.101 vol.%. In N Germany, the concentration is 0.0124 vol.%, and in the Solway Basin (UK), the maximum content is 0.0026 vol.%. The Spathian sedimentary record of French and English successions shows no fossil remains, only some signs of bioturbation in the Vosges Mountains (NE France) (Bourquin *et al.* 2009) and possible vertebrate footprints in the Solway Basin (Brookfield, 2004) in the middle Spathian sedimentary record. However, the German succession for these ages contains plant remains, conchostracans and acritarchs (Aigner and Bachmann, 1992). This decreasing trend in APS mineral content continues northwards, and the Boreal area (Barents Sea, Norway) (Rossi *et al.* 2019) is practically devoid of APS minerals. In contrast to areas at lower latitudes, temperature and acidity conditions in the Boreal area were not as extreme during the SSB (Woods, 2005). So, even though paleontological evidence indicates a synchronous major change in terrestrial and marine ecosystems near the SSB, this area might be regarded as a most likely refuge of plants and of early recovery during the Early Triassic (Galfetti *et al.* 2007), allowing deciduous forests and temperate paleosols (Retallack *et al.* 2011).

As in the Boreal areas, virtually no APS minerals have been found in the southern high-latitude studied sections of South Africa and E Australia during the SSB (Figure 4 and

https://doi.org/10.1017/S0016756825100472 Published online by Cambridge University Press

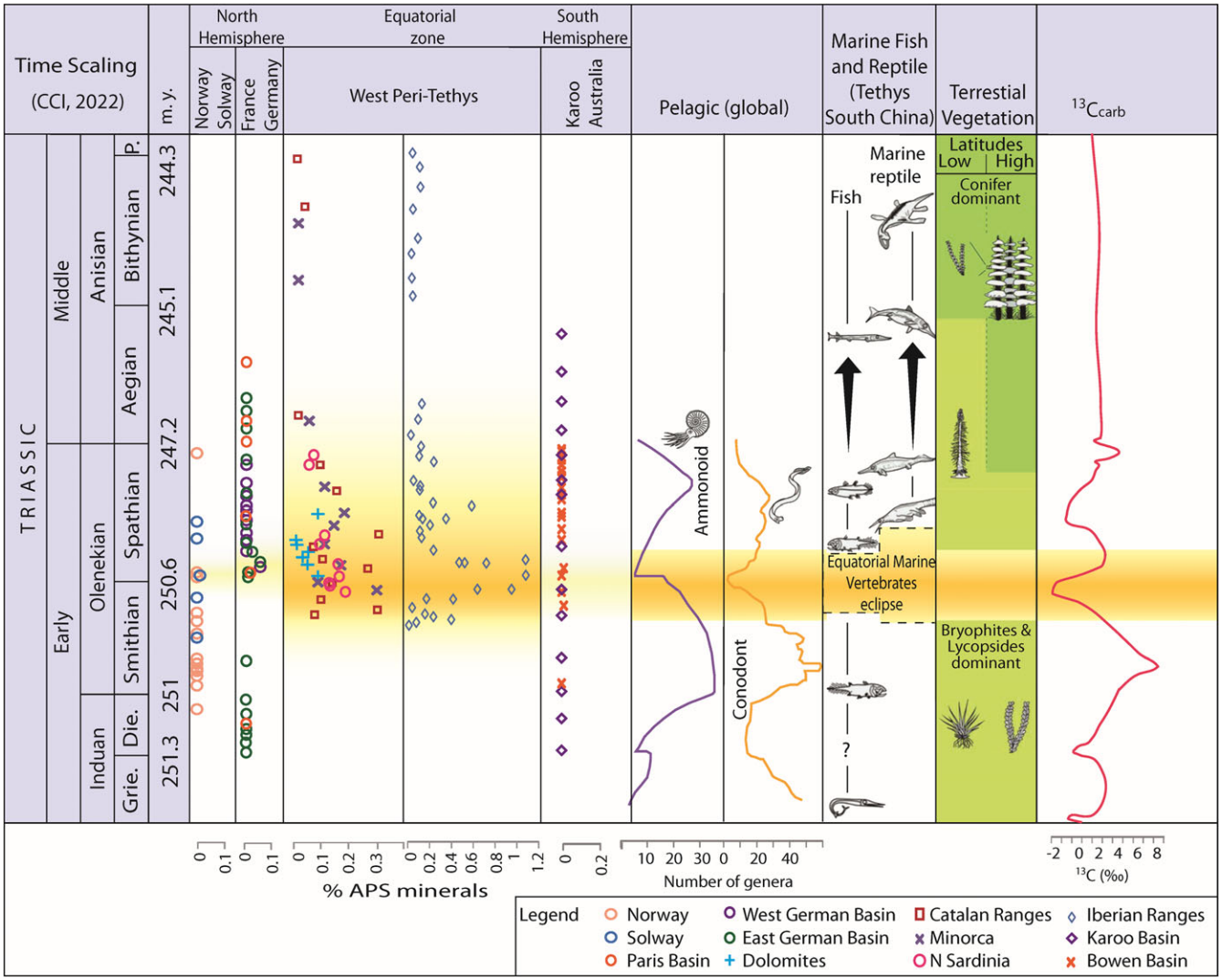

Figure 4. Volume fraction of APS minerals across the studied sections (this study) together with biotic ammonoid and conodont (Stanley, 2009) and flora (Hochuli et al. 2016) changes and simplified carbon isotope signatures (Payne et al. 2004) during the Early and Middle Triassic. For the sake of clarity, volume fraction of APS minerals data from equatorial latitudes has been split into two separate columns, one for the Iberian Ranges and another for the Catalan Ranges, Minorca, N Sardinia and Dolomites. (See Supplementary Table S2 for complementary information).

Supplementary Table S2). In these areas, the presence of different types of fossils (Smith and Botha-Blink, 2014; Retallack, 2021) shows that the consequences of damaged environmental conditions were not as marked as in low latitudes. The chemical composition of paleosols and stomatal index of fossil plants in the Bowen Basin, E Australia, reveals this CO_2 crisis coincided with elevated temperatures and precipitation, but also with opportunities for transient migrations of lycopsids and large amphibians to higher latitudes (Retallack *et al.* 2011). During the middle Smithian, *Dicroidium* leaves and dispersed cuticles become common in the central Sydney Basin (65°–70°S) and persisted throughout the remainder of the Triassic in E Australia, becoming a dominant component of coal-forming mire ecosystems in the Middle and Late Triassic (Fielding *et al.* 2019).

Our results are consistent with global patterns of biotic activity documented during the Early Triassic, although the differences between the mechanisms and effects operating in marine and continental realms must be taken into account. At the end-Smithian, there were major losses in many marine groups, including bivalves, conodonts and ammonoids (Stanley, 2009). Fish fossils are very rare in equatorial areas, especially in the Smithian successions, despite being common at higher latitudes at the time (Sun *et al.* 2012). Marine reptile fossils (ichthyosaur) are also not found in equatorial waters until the middle-late Spathian (Sun *et al.* 2012). Other notable absences from equatorial oceans are calcareous algae during the entire end-Permian–early Spathian interval, although they are present in higher latitudes (Wignall *et al.* 1998). The increase in temperature and acidity in the oceans has a direct relationship with the atmospheric increase in CO_2 (Wignall, 2011).

On land, tetrapod fossil occurrences are generally absent between 30°N and 40°S during the Early Triassic (Romano *et al.* 2020). Moreover, in equatorial Pangea, conifer-dominated forests did not become established until the end of the Spathian (Looy *et al.* 1999). The interval between the end of the Smithian and the end of the Spathian, during which acidic conditions prevailed, coincides with a phase of global warming (Bourquin *et al.* 2011). The ultimate causes of global acidification remain uncertain, but

https://doi.org/10.1017/S0016756825100472 Published online by Cambridge University Press

the most plausible explanation involves the environmental impact of aerosols generated by STM activity (Payne *et al.* 2004), which would have produced acid rain (Black *et al.* 2014) and contributed to widespread continental acidification (Galfetti *et al.* 2007). The massive injection of CO_2 into the atmosphere associated with Siberian volcanism is considered to have driven this global warming (Hochuli *et al.* 2016) and to have sustained episodes of acid rainfall with comparable effects in both hemispheres, as modelled by Black *et al.* (2014) for the EPME. These authors also emphasized that acid rain and the global collapse of the ozone layer, linked to episodic pyroclastic volcanism and heating of volatile-rich Siberian country rocks, generated repeated and rapidly imposed atmospheric stresses that contributed to terrestrial ecological collapse. Sulphur injected during these eruptions can sharply decrease pH once eruptive activity ceases. The mechanisms inferred for the EPME likely remained active during the Early Triassic pulses (Svensen *et al.* 2009), thereby delaying biotic recovery until the SSB. We suggest that APS mineral precipitation is closely related to these recurrent episodes of sulphur injection into the atmosphere. According to the model of Black *et al.* (2014), enhanced acidity in equatorial regions is likely governed by wind circulation patterns and regional precipitation totals. The configuration of the Pangean landmass during the Early Triassic may have disrupted zonal circulation (Kutzbach and Gallimore 1989), and seasonal temperature contrasts between hemispheres may have produced pressure gradients that drove cross-equatorial airflow (Parrish, 1993). These conditions may have facilitated the migration of volcanic aerosols from the STM towards lower latitudes during the SSB, where surface acidity and associated environmental impacts intensified. Acid rain derived from sulphate aerosols would have been particularly strong in the Northern Hemisphere, with its most pronounced effects between the equator and 60°N (Black *et al.* 2014). This is likely because acid gases (HF, HCl and SO_2) are attenuated during long-distance transport, which may help explain the scarcity of APS minerals in Southern Hemisphere sections.

Although arid climatic conditions may have contributed to sustaining environmental acidity, the presence of APS minerals in the study areas does not depend exclusively on climatic variability. During the arid pulse at the end of the Spathian, no increase in APS minerals is observed; the establishment of a semi-arid climate took place only after APS concentrations had already declined.

Our study offers an approach for estimating acidity in continental sequences and for evaluating its impact on environmental change and ecosystem recovery. Acidity contributed to the SSB biotic crisis and moderated the recovery after the EPME, with variable impacts on Pangea ecosystems depending on their paleolatitude. The high APS contents at the SSB in equatorial areas strongly suggest that pulses of highly acidic conditions conducive to APS formation likely persisted for longer and were more intense than those recorded in higher latitude sections.

The Early Triassic provides a unique deep-time perspective on the precarious balance between life and acid conditions depicted during SSB major environmental changes. The APS distribution across global continental records confirms acidity levels during the SSB were decisive for the onset of life recovery after the EPME. Acidity levels were conditioned by latitude, with the SSB biotic crisis having lower environmental impact in high latitudes, where recovery was therefore faster. Acidic conditions did not return to SSB levels during the Middle Triassic, allowing environmental recovery after the EPME.

Supplementary material. The supplementary material for this article can be found at https://doi.org/10.1017/S0016756825100472

Acknowledgements. The authors acknowledge the Exploration Data Centre of the Department of Resources, Queensland Government (Australia), for assistance in core retrieval, investigation and sampling, and the Norwegian Petroleum Directorate for permission to sample well 7226 11-1. They also appreciate the technical assistance of the National Center for Electron Microscopy (Madrid) for EMPA and SEM analysis. Constructive criticism from an anonymous reviewer helped to improve the manuscript.

Financial support. The authors are grateful for the financial support of the projects PID2022-141050NB-I00 (Spain), PRIN 2022–24 (Italy) and ARC FT230100230 (Australia).

Competing interests. The authors have no competing interests as defined by the journal or other interests that might be perceived to influence the results and/or discussion reported in this paper.

Author contributions. JFB and JLG: Original proposal and coordination of the study. Field work and sample collection in the Iberian Ranges, Catalonia, Minorca (Spain), Sardinia, Dolomites (Italy), West and East German Basins (Germany) and Bowen Basin (Australia). Drafting of the manuscript and drawing of figures. VBA: Field work and sample collection in the Iberian Ranges, Minorca (Spain), Sardinia and Dolomites (Italy). Determination of APS mineral content by EMPA. Drafting of the manuscript and drawing of figures. ABGA: Field work and sample collection in the Iberian Ranges and Catalonia (Spain) and West German Basin (Germany). Discussion and input on the draft manuscript. FJL: Sample processing and mineralogical study. Discussion and input on the draft manuscript. RHB: Field work and sample collection in the Iberian Ranges, Minorca, Catalonia (Spain), Sardinia and Dolomites (Italy). Discussion and input on the draft manuscript. TU and JE: Field work and sample collection in the Bowen Basin (Australia). Discussion and input on the draft manuscript. AR: Field work and sample collection in the Nurra Basin (Sardinia, Italy). Discussion and input on the draft manuscript. PG: Field work and sample collection in the Dolomites (Italy). Discussion and input on the draft manuscript. NP y VMR: Sample collection in the Western and NW Barents Sea (Norway). Discussion and input on the draft manuscript. TMC: Field work and sample collection in the East German Basin (Germany). Discussion and input on the draft manuscript. RMHS and DW: Field work and sample collection in the Central Karoo Basin (South Africa). Discussion and input on the draft manuscript. SB: Sample collection in the Vosges Mountains (France). Discussion and input on the draft manuscript. MB: Field work and sample collection in the Solway Basin (UK). Discussion and input on the draft manuscript.

Data availability statement. Data are provided within the manuscript or supplementary information files.

References

Aigner T. and Bachmann G. H (1992) Sequence-stratigraphic framework of the German Triassic. *Sedimentary Geology* **80**, 115–135.

Arche A. and López-Gómez J (2005) Sudden changes in fluvial style across the Permian-Triassic boundary in the Eastern Iberian Ranges, Spain: analysis of possible causes. *Palaeogeography, Palaeoclimatology, Palaeoecology* **229**, 104–126.

Bachmann G.H. and Kozur H.W (2004) The Germanic Triassic: correlation with the international chronostratigraphic scale, numerical ages and Milankovitch cyclicity. *Hallesches Jahrbuch Geowiss* **B26**, 17–62.

Balme B, Kershaw A and Webb J (1995) Floras of Australian coal measures with notes on their associated Mesozoic faunas. In *Geology of Australian Coal Basins* (eds CR Ward, HJ Harrington, CW Mallett and JW Beetson), pp. 41–62. Geological Society of Australia Incorporates, Coal Geology Groups.

Barrenechea JF, Gianolla P, López-Gómez J, Borruel-Abadía V, De La Horra R and Ronchi A (2025) Environmental implications of the mineralogical record in Olenekian (Early Triassic) units in Western Dolomites (Italy):

acidity conditions and ecosystems recovery. *Journal of Iberian Geology*. https://doi.org/10.1007/s41513-025-00317-6.

Baucon A, Ronchi A, Felletti F & De Carvalho CN (2014) Evolution of Crustaceans at the edge of the end-Permian crisis: ichnonetwork analysis of the fluvial succession of Nurra (Permian–Triassic, Sardinia, Italy). *Palaeogeography, Palaeoclimatology, Palaeoecology* **410**, 74–103.

Black BA., Lamarque JF, Shields CA, Elkins-Tanton LT and Kiehl JT (2014) Acid rain and ozone depletion from pulsed Siberian Traps magmatism. *Geology* **42**, 67–70.

Borruel-Abadía V, López-Gómez J, De La Horra R, Galán-Abellán B, Barrenechea JF, Arche A, Ronchi A, Gretter N and Marzo M (2015) Climate changes during the Early–Middle Triassic transition in the E. Iberian plate and their palaeogeographic significance in the western Tethys continental domain. *Palaeogeography, Palaeoclimatology, Palaeoecology* **440**, 671–689.

Borruel-Abadía V, Barrenechea JF, Galán-Abellán AB, Alonso-Azcárate J, De La Horra R, Luque FJ and López-Gómez J (2016) Quantifying aluminium phosphate–sulphate minerals as markers of acidic conditions during the Permian–Triassic transition in the Iberian Ranges, E Spain. *Chemical Geology* **429**, 10–20.

Borruel-Abadía V, Barrenechea JF, Galán-Abellán AB, De La Horra R, López-Gómez J, Ronchi A, Luque FJ, Alonso-Azcárate J and Marzo M (2019) Could acidity be the reason behind the early Triassic biotic crisis on land? *Chemical Geology* **515**, 77–86.

Bourquin S, Péron S and Durand M (2006) Lower Triassic sequence stratigraphy of the western part of the German Basin (west of Black Forest): Fluvial system evolution through time and space. *Sedimentary Geology* **186**, 187–211.

Bourquin S, Guillocheau F and Péron S. (2009) Braided rivers within an arid alluvial plain (example from the Lower Triassic, western German Basin): recognition criteria and expression of stratigraphic cycles. *Sedimentology* **56**, 2235–2264.

Bourquin S, Bercovici A, López-Gómez J, DIEZ J. B, Broutin J, RONCHI A, Durand M, Arché A, Linol B and Amour, F (2011) The Permian–Triassic transition and the onset of Mesozoic sedimentation at the Northwestern peri-Tethyan domain scale: Palaeogeographic maps and geodynamic implications. *Palaeogeography, Palaeoclimatology, Palaeoecology* **299**, 265–280.

Broglio Loriga C (1986) The early macrofaunas of the Werfen formation and the Permian-Triassic boundary in the Dolomites (Southern Alps, Italy). *Studi Trentini di Scienze Naturali - Acta Geologica* **62**, 3–18.

Brookfield ME (2004) The enigma of fine-grained alluvial basin fills: the Permo-Triassic (Cumbrian Coastal and Sherwood Sandstone Groups) of the Solway Basin, NW England and SW Scotland. *International Journal of Earth Sciences* **93**, 282–296.

Brookfield, ME (2008) Palaeoenvironments and palaeotectonics of the arid to hyperarid intracontinental latest Permian-late Triassic Solway basin (U.K.). *Sedimentary Geology* **210**, 27–47.

Cassinis G, Durand M and Ronchi A (2003) Permian-Triassic continental sequences of Northwest Sardinia and South Provence: stratigraphic correlations and palaeogeographical implications. *Bollettino della Società Geologica Italiana* **2**, 119–129.

Cassinis G, Perotti C. and Ronchi A (2012) Permian continental basins in the Southern Alps (Italy) and peri-mediterranean correlations. *International Journal of Earth Sciences* **101**, 129–157.

Cohen KM, Finney SC, Gibbard PL and Fan JX (2013) The ICS International Chronostratigraphical Chart. *Episodes* **36**, 199–204.

Dal Corso J, Newton RJ, Zerkle AL, Chu D, Song H, Song H, Tian L, Tong J, Di Rocco T, Claire MW, Mather TA, He T, Gallagher T, Shu W, Wu Y, Bottrell SH, Metcalfe I, Cope H A, Novak M, Jamieson RA and Wignall PB (2024) Repeated pulses of volcanism drove the end-Permian terrestrial crisis in northwest China. *Nature Communications* **15**, 7628.

Dill HG (2001) The geology of aluminium phosphates and sulphates of the alunite group minerals: A review. *Earth-Science Reviews* **53**, 35–93.

Fielding CR, Frank TD, Mcloughlin S, Vajda V, Mays C, Tevyaw AP, Winguth A, Winguth C, Nicoll RS and Bocking M (2019) Age and pattern of the southern high-latitude continental end-Permian extinction constrained by multiproxy analysis. *Nature communications* **10**, 385.

Galán-Abellán AB, Barrenechea JF, Benito MI, De La Horra R, Luque J, Alonso-Azcárate J, Arche A, López-Gómez J and Lago, M. (2013a) Palaeoenvironmental implications of aluminium phosphate-sulphate minerals in Early–Middle Triassic continental sediments, SE Iberian Range (Spain). *Sedimentary Geology* **289**, 169–181.

Galán-Abellán AB., Alonso-Azcárate J, Newton RJ, Bottrell SH, Barrenechea JF, Benito MI, De La Horra R, López-Gómez J and Luque J (2013b) Sources of Sr and S in aluminum-phosphate-sulfate minerals in early–middle Triassic sandstones (Iberian Ranges, Spain) and paleoenvironmental implications for the west Tethys. *Journal of Sedimentary Research* **83**, 406–426.

Galfetti T, Hochuli PA, Brayard A, Bucher H, Weissert H and Vigran JO (2007) Smithian-Spathian boundary event: evidence for global climatic change in the wake of the end-Permian biotic crisis. *Geology* **35**, 291–294.

Glørstad-Clark E, Feleide JL, Lundschein B and Nystuen JP (2010) Triassic seismic sequence stratigraphy and paleogeography of the western Barents Sea area. *Marine and Petroleumgeology* **27**, 1448–1475.

Glørstad-Clark E, Birkeland E, Nystuen J, Faleide J and Midtkandal I (2011) Triassic platform-margin deltas in the western Barents Sea: *Marine and Petroleum Geology* **28**, 1294–1314.

Hand E (2015) Acid oceans cited in Earth's worst die-off. *Science* **348**, 165–166.

Hammer O, Jones MT, Scheebeli-Hermann E and Hansen BB (2019) Are early Triassic extinction events associated with mercury anomalies? A reassessment of the Smithian/Spathian boundary extinction. *Earth-Science Review* **195**, 179–190.

Hochuli PA, Sanson-Barrera A, Schneebeli-Hermann E and Bucher H (2016) Severest crisis overlooked—Worst disruption of terrestrial environments postdates the Permian–Triassic mass extinction. *Scientific Reports* **6**, 1–7.

Hounslow MW and Mcintosh G (2003) Magnetostratigraphy of the Sherwood Sandstone Group (Lower and Middle Triassic), south Devon, UK: detailed correlation of the marine and non-marine Anisian. *Palaeogeography, Palaeoclimatology, Palaeoecology* **193**, 325–348.

Kutzbach J and Gallimore R (1989) Pangaean climates: megamonsoons of the megacontinent: Journal of Geophysical Research. *Atmospheres* **94**, 3341–3357.

Li M, Frank TD, Xua Y, Fielding CR, Gong Y. and Shen Y (2022) Sulfur isotopes link atmospheric sulfate aerosols from the Siberian Traps outgassing to the end-Permian extinction on land. *Earth and Planetary Science Letters* **592**, 117634.

Liu F, Peng H, Marshall JE, Lomax BH, Bomfleur B, Kent MS, Fraser WT and Jardine PE (2023) Dying in the sun: direct evidence for elevated UV-B radiation at the end-Permian mass extinction. *Science Advances*, **9**, eabo6102.

Looy C, Brugman W, Dilcher D and Visscher H (1999) The delayed resurgence of equatorial forests after the Permian–Triassic ecologic crisis. *Proceedings of the national Academy of Sciences* **96**, 13857–13862.

Mays C, Vajda V, Frank TD, Fielding CR, Nicoll RS, Tevyaw AP and Mcloughlin S (2020) Refined Permian–Triassic floristic timeline reveals early collapse and delayed recovery of south polar terrestrial ecosystems. *GSA Bulletin* **132**, 1489–1513.

Metcalfe I, Crowley J, Nicoll R and Schmitz M (2015) High-precision U-Pb CA-TIMS calibration of Middle Permian to Lower Triassic sequences, mass extinction and extreme climate-change in eastern Australian Gondwana. *Gondwana Research* **28**, 61–81.

Orchard MJ (2007) Conodont diversity and evolution through the latest Permian and Early Triassic upheavals. *Palaeogeography, Palaeoclimatology, Palaeoecology* **252**, 93–117.

Parrish JT (1993) Climate of the supercontinent Pangea. *The Journal of Geology* **10**, 215–233.

Paterson NW, Rossi VM and Schneebeli-Hermann E (2024) Volcanogenic mercury and plant mutagenesis during the end-Permian mass extinction: palaeoecological perturbation in northern Pangaea. *Gondwana Research* **134**, 123–143.

Payne JL, Lehrmann DJ, Wei J, Orchard MJ, Schrag DP and Knoll AH (2004) Large perturbations of the carbon cycle during recovery from the end-Permian extinction. *Science* **305**, 506–509.

Péron S, Bourquin S, Fluteau F and Guillocheau F (2005) Paleoenvironment reconstructions and climate simulations of the Early Triassic: impact of the water and sediment supply. *Comptes Rendus Palevol* **4**, 555–568.

Posenato R. (2019) The end-Permian mass extinction (EPME) and the Early Triassic biotic recovery in the western Dolomites (Italy): state of the art. *Bollettino della Società Paleontologica Italiana* **58**, 11–34.

Retallack GJ (2021) Multiple Permian-Triassic life crises on land and at sea. *Global and Planetary Change* **198**, 103415.

Retallack GJ, Smith RMH and Ward PD (2003) Vertebrate extinction across the Permian-Triassic boundary in the Karoo Basin of South Africa. *Bulletin of the Geological Society of America* **115**, 1133–1152.

Retallack GJ, Sheldon ND, Carr PF, Fanning M, Thompson CA, Williams ML, Jones BG. and Hutton A (2011) Multiple early Triassic greenhouse crises impeded recovery from Late Permian mass extinction. *Palaeogeography, Palaeoclimatology, Palaeoecology* **308**, 233–251.

Romano M, Bernardi M, Petti FM, Rubidge B, Hancox J and Benton MJ (2020) Early Triassic terrestrial tetrapod fauna: a review. *Earth-Science Reviews* **210**, 103331.

Ronchi A. (2001) Upper Paleozoic and Triassic continental deposits of Sardinia: A stratigraphic synthesis. In *Permian Continental Deposits of Europe and Other Areas: Regional Reports and Correlations*(Ed G Cassinis), vol. **25**, pp. 139–148. Natura Bresciana. Museo Civicodi Scienze Naturali de Brescia.

Rossi VM, Paterson NW, Helland-Hansen W, Klausen TG and Eide CH (2019) Mud-rich delta-scale compound clinoforms in the Triassic shelf of northern Pangea (Havert Formation, south-western Barents Sea). *Sedimentology* **66**, 2234–2267.

Sahney S and Benton MJ (2008) Recovery from the most profound mass extinction of all time. *Proceedings of the Royal Society B: Biological Sciences* **275**, 759–765.

Smith, RMH. and Botha-Blink J (2005) The recovery of terrestrial vertebratediversity in the South African Karoo Basin after the end-Permian extinction. *Comptes Rendus Palevol* **4**, 623–636.

Smith RM and Botha-Blink J (2014) Anatomy of a mass extinction: sedimentological and taphonomic evidence for drought-induced die-offs at the Permo-Triassic boundary in the main Karoo Basin, South Africa. *Palaeogeography, Palaeoclimatology, Palaeoecology* **396**, 99–118.

Smith RMH and Ward PD. (2001) Pattern of vertebrate extinctions across an event bed at the Permian–Triassic boundary in the Karoo Basin of South Africa. *Geological Society of America* **29**, 1147–1150.

Stanley SM (2009) Evidence from ammonoids and conodonts for multiple Early Triassic mass extinctions. *Proceedings of the National Academy of Sciences* **106**, 15264–15267.

Stoffregen RE and Alpers CHN (1987) Woodhouseite and svanbergite in hydrothermal ore deposits: Products of apatite destruction during advanced argillic alteration. *The Canadian Mineralogist* **25**, 201–211.

Sun Y, Joachimski MM, Wignall PB, Yan C, Chen Y, Jiang H, Wang L and Lai X (2012) Lethally hot temperatures during the Early Triassic greenhouse. *Science* **338**, 366–370.

Svensen H, Planke S, Polozov AG, Schmidbauer N, Corfu F, Podladchikov YY and Jamtveit B (2009) Siberian gas venting and the end Permian environmental crisis. *Earth and Planetary Science Letters* **27**, 490–500.

Szurlies M (2007) Latest Permian to Middle Triassic cyclo-magnetostratigraphy from the Central European Basin, Germany: implications for the geomagnetic polarity timescale. *Earth and Planetary Science Letters* **261**, 602–619.

Vieillard P, Tardy Y and Nahon D (1979) Stability fields of clays and aluminum phosphates: parageneses in lateritic weathering of argillaceous phosphatic sediments. *American Mineralogist* **64**, 626–634.

Vigram JO, Mangerud G, Mork A, Worsley D, Hochuli PA (2014) *Palynology and Geology of the Triassic Succession of Svalvard and the Barents Sea*. vol. **14**, p. 274. Throndheim: Geological Survey of Norway Special Publication.

Voigt T and Gaupp R (2000) Die fazielle Entwicklung an der Grenze zwischen Unterem und Mittlerem Buntsandstein im Zentrum der Thüringer Senke. *Beiträge Geologie Thüringen, N. F.* **7**, 55–71.

Wignall PB, (2011) Lethal volcanism. *Nature* **477**, 285–286.

Wignall P, Morante R and Newton R (1998) The Permo-Triassic transition in Spitsbergen: δ13Corg chemostratigraphy, Fe and S geochemistry, facies, fauna and trace fossils. *Geological Magazine* **135**, 47–62.

Woods AD (2005) Paleoceanographic and paleoclimatic context of Early Triassic time. *Comptes Rendus Palevol* **4**, 463–472.

Wu Q, Zhang H, Ramezani J, Zhang FF, Erwin DH, Feng Z, Shao LY, Cai YF, Zhang SH, Xu YG and Shen SH (2024) The terrestrial end-Permian mass extinction in the paleotropics postdates the marine extinction. *Science Advances* **10**, 7284.

https://doi.org/10.1017/S0016756825100472 Published online by Cambridge University Press